Mechanical Properties of an Extremely Tough 1.5 mol% Yttria Stabilized Zirconia Material

Frank Kern * and Bettina Osswald

Posted Date: 15 July 2024

doi: 10.20944/preprints202407.1207.v1

Keywords: zirconia; mechanical properties; transformation toughening; microstructure

Article

Mechanical Properties of an Extremely Tough 1.5 mol% Yttria Stabilized Zirconia Material

Frank Kern * and Bettina Osswald

Institute for Manufacturing Technologies of Ceramic Components and Composites, Faculty 7: Engineering Design, Production Engineering and Automotive Engineering, University of Stuttgart, Allmandring 7b, 70569 Stuttgart, Germany

* Correspondence: frank.kern@ifkb.uni-stuttgart.de

Abstract: Yttria stabilized zirconia (Y-TZP) ceramics with drastically reduced yttria content have been introduced by different manufacturers aiming at improving the damage tolerance of ceramic components. In this study an alumina doped 1.5Y-TZP was axially pressed, pressureless sintered in air at 1250–1400 °C for 2 h and characterized with respect to mechanical properties, microstructure and phase composition. The material exhibits a combination of high strength of 1000 MPa and a high toughness of 8.5–10 MPa√m. The measured fracture toughness is, however, extremely depending on measurement protocol. Direct crack length measurements overestimate toughness due to trapping effects. The initially purely tetragonal material has a high transformability of > 80 %, the transformation behavior is predominantly dilatoric, measured R-curve related toughness increments are in good agreement with transformation toughness increments derived from XRD data.

Keywords: zirconia; mechanical properties; transformation toughening; microstructure

1. Introduction

Ceramics are inherently brittle materials. In the absence of R-curve effects, their strength σ *a priori* depends on the fracture toughness K_{IC} and the defect size a ($\sigma = K_{IC}/\sqrt{(\pi a)}$). Improving the strength of ceramic components is therefore a matter of sophisticated processing (compounding, shaping, sintering, machining) to reduce defect size and material science to develop materials with higher toughness. According to Evans the total toughness is determined by the combination of the intrinsic toughness K_0 and the sum of the toughness increments K_i introduced by different reinforcements effects ($K_{IC} = K_0 + \Sigma K_i$) [1].

In partially stabilized zirconia materials the dominant reinforcement effect is transformation toughening, a stress-induced martensitic transformation of metastable tetragonal phase to stable monoclinic phase associated with volume expansion and shear [2]. The phase transformation is triggered at the tip of a crack under tensile stress. As the crack proceeds, the compressive stresses on both sides of the crack resulting from transformation induced volume expansion close the crack and thereby reduce the stress intensity at the crack tip [3].

In order to retain the metastable tetragonal phase after sintering, stabilizer oxides are added which form solid solutions with zirconia and stabilize the high temperature phase by expanding the lattice (oversize dopants) with cation radius $r_c > r(Zr^{4+})$ and/or by introduction of oxygen vacancies (aliovalent cations such as Y^{3+} or other trivalent rare earth cations) [4,5]. The second prerequisite to retain the tetragonal phase metastable is a sufficiently fast cooling after sintering.

Depending on the type and amount of stabilizer oxide the partially stabilized zirconia materials (either entirely tetragonal as TZP = tetragonal zirconia polycrystals or as tetragonal precipitates in a cubic matrix PSZ = partially stabilized zirconia) show different features concerning strength and toughness. Yttria stabilized zirconia, which is frequently applied in mechanical engineering and biomedical, is typically stabilized with 3 mol-% Y_2O_3 (3Y-TZP) and has high strength of > 1000 MPa but moderate toughness of ~5 MPa√m [6]. Ceria stabilized zirconia (with ~12 mol-% CeO_2 = 12 Ce-

 doi:10.20944/preprints202407.1207.v1

TZP) has high toughness but only moderate strength [7]. The stabilizer cations also effect the transformation behavior of the TZP material. In Ce-TZP the large tetravalent ceria cations expand the zirconia lattice (which leads to a minor lattice distortion) but do not introduce oxygen vacancies. Ce-TZP therefore tends to transform in a cooperative (autocatalytic) manner, as due to the high symmetry of the lattice, the monoclinic lamella can easily trigger the transformation of adjacent grains [8]. Stress strain curves of tough Ce-TZP materials show characteristics analogous to work-hardening in metals. The autocatalytic or burst transformation is interrupted when the remaining tetragonal domains are locally separated by transformed material or a second phase, i.e. when the transformation is exhausted [9,10]. Ce-TZP materials are typically very tough, but autocatalytic transformation is not very efficient [11]. It is noteworthy that in Ce-TZP there is significant transformation before the crack tip and not only in the wake of the crack. Such materials show R-curve or transformation dominated failure, i.e. the material transforms prior to crack growth.

In yttria stabilized zirconia, the trivalent dopants introduce oxygen vacancies for charge neutrality, reduce the coordination number of zirconium cations and thereby distort the zirconia lattice significantly [8]; additionally there is a moderate contribution by lattice expansion. The symmetry reduction leads to a more localized transformation behavior. Individual grains with the right size and orientation to the applied stress transform. The transformation is predominantly dilational; burst transformation is not observed. This leads to materials with moderate toughness but a very steep R-curve [12]. The plateau toughness is reached after a few micrometers crack length. This behavior makes Y-TZP materials attractive for small and mechanically highly loaded components.

According to McMeeking and Evans (equation 1) [13], the two important parameters which govern the transformation toughness ΔK_{IC}^{T} are the transformability V_f and the size of the transformation zone h. All other parameters such as υ = Poisson's ratio, E = Young's modulus and ε_T = transformation strain are material constants. The parameter X describes the transformation characteristics, X = 0.22 for purely dilational transformation and 0.48 for dilation and shear. Y-TZP has a predominantly dilational transformation characteristics (X = 0.27) [12].

$$\Delta K_{IC}^{T} = X/(1-\upsilon) \cdot \varepsilon_T \cdot E \cdot V_f \cdot \sqrt{h} \qquad (1)$$

The transformability of a tetragonal grain depends on its size, its stabilizer content and the constraint of the surrounding matrix [14]. In order to increase the toughness of Y-TZP, either larger grain sizes are produced by increasing the firing temperature or the stabilizer content is reduced [15,16]. Thus, for a given stabilizer content a critical grain size exists above which spontaneous transformation during cooling is observed. The lower the stabilizer content the smaller the critical grain size [17]. Thermodynamically, reduction of stabilizer content has another implication, the t/t+c phase boundary at typical sintering temperatures of ~1400°C is located at 2.5 mol-% Y_2O_3 [18]. Materials made from coprecipitated Y-TZP powders with yttria contents above this limit are supersaturated with yttria. Complete segregation of cubic phase, however, requires high sintering temperature and prolonged sintering [19]. Materials with yttria contents lower than 2.5 mol-% are entirely tetragonal. Yttria segregation to grain boundaries is less pronounced than in 3Y-TZP. Hence, their grain growth is not retarded to the same extent. Moreover, such materials are potentially more prone to low temperature degradation (LTD) due to their low yttria content and the moderate segregation of the stabilizer to the grain boundaries. Low-yttria Y-TZP materials therefore typically require very fine grain starting powders with excellent sinterability to obtain fully dense and fine grain sintered Y-TZP.

Y-TZP materials from powders with less than 2 mol-% yttria are well documented in scientific literature. Toughness values achieved in these lab-scale studies were considerable [20,21]. However, until recently few reproducible and processible ultrafine powders were available. The practical application of extremely understabilized Y-TZP was probably considered too dangerous with respect to spontaneous phase transformation and component failure. Today, fine grain Y-TZP powders with yttria contents between 1.5–2 mol-% are available from different manufacturers in reproducible quality and are provided not only as plain powders but also as ready-to-press (RTP) granulate formulations. Concerning the Tosoh ZGAIA 1.5YHT RTP powder used in this study, a first publication by Matsui [22] gave information about the suitable sintering temperature range (≤ 1400

 doi:10.20944/preprints202407.1207.v1

°C/1 h), indicated a homogeneous stabilizer distribution, reported an extremely high toughness (> 20 MPa√m, measured by indentation) and high bending strength of 1300 MPa (3pt bending). With respect to the experimental database of strength toughness correlations compiled by Swain [12], this extreme toughness combined with a high strength was questionable. In another study on the same material, Imariouane [23] confirmed high strength and a lower but still very considerable toughness of 8.5 MPa√m (SEVNB method), which is within the theoretically accepted limits. They showed transformation bands indicating transformation induced failure, yet no non-linearity in the stress-strain curves. Susceptibility towards LTD seems moderate. In a second paper the sensitivity to sintering conditions was highlighted, slow cooling leads to LTD in presence of ambient moisture and does not require presence of hot water or steam [24]. A summary of strength and toughness of various 1.5-2Y-TZP materials using different measurement protocols is given in [25].

In the present paper we attempt to understand more about the transformation behavior and failure characteristics of 1.5Y-TZP and clarify why direct crack length measurements lead to drastically overestimated toughness values. Finally, we tried to elaborate a reliable indentation based protocol to measure fracture toughness for fine grained and transformable TZP.

2. Materials and Methods

The powder used in this study was spray granulated ready-to-press (RTP) powder provided by the manufacturer (ZGAIA 1.5HT, Tosoh, Tokio, Japan). According to the data sheet, the powder is stabilized with 1.5 mol-% Y_2O_3, 0.3 vol% of alumina is added as a sintering aid. The powder is the same as in [22,23].

Quadratic plates of 35 x 35 mm² size and 2.5 mm thickness were pressed using a manually operated uniaxial hydraulic press (Paul Weber, Remshalden, Germany). The stainless steel die has rounded corners and double sided punches. The applied load was 150 kN corresponding to 125 MPa pressure. 9 g of RTP powder was weighed for each sample and 16 plates were manufactured with identical pressing parameters.

The plates were subsequently de-bindered in air (60 °C/h to 600 °C, 3 h dwell, free cooling). Four plates per sintering temperature were then sintered in a dental furnace at 1250 °C, 1300 °C, 1350 °C and 1400 °C (MIHM-Vogt HT speed, Stutensee, Germany). Heating was performed with 2 °C/min to 1200 °C and then with 1 °C/min to final sintering temperature, the dwell was 2 h, then the samples were cooled with the maximum cooling speed possible.

The sintered plates were then manually beveled with a 40 µm diamond disk and glued on sample holders. Machining included automatic lapping with 15 µm diamond suspension (Struers Rotopol, Copenhagen, Denmark) on both sides. One side was polished for 30 min each using 15 µm, 6 µm, 3 µm and 1 µm diamond suspension to obtain a mirror-like surface. After machining the thickness of the plates was 2 ± 0.1 mm.

The plates were cut into bending bars of 4 mm width using a diamond wheel (Struers Accutom, Copenhagen, Denmark). The as-cut bars were lapped on the sides to remove the cutting grooves and beveled at the edges.

Mechanical testing included Vickers hardness measurements (five HV10 indents per sample, 98.1 N, Bareiss, Oberdischingen, Germany), the Young's modulus was assumed to be 210 GPa, which is the typical values for fully dense Y-TZP. Bending strength was performed in a 4-pt setup with 20 mm outer and 10 mm inner span, the crosshead speed was set to 0.5 mm/min (Zwick, Ulm, Germany, 10 samples). Up to three bars were tested in a 3pt setup to eventually create transformation bands which allow to determine transformation stress. The transformation stress σ_T can be calculated from the distance of the first transformation bands d divided by the span length l and the failure stress ($\sigma_T = \sigma_F \cdot d/l$) [26].

As data on fracture toughness of this material are controversial in literature, various toughness measurement protocols were applied. Indentation toughness measurements with direct crack length measurement K_{DCM} were performed to reproduce Matsui's measurements [22]. On the leftover pieces of sample cutting as many indents (typically ~20 per sample) were placed to collect 20 valid wing crack length values (due to crack trapping in the transformation zone around the indents most HV10

 doi:10.20944/preprints202407.1207.v1

indents only produce 1-2 wing cracks, fully valid crack patterns were rare). The indentation toughness K_{DCM} was then calculated using the formula of Niihara et. al assuming Palmqvist type cracks [27].

Four bars were notched with four indents each on the polished tensile side for toughness measurements by indentation strength in bending (K_{ISB}). The cracks were placed at a distance of 2 mm so that they all fit within the inner span of the above mentioned 4pt setup. Cracks of the indents were oriented parallel and perpendicular to the sample sides. Four indents were placed to compensate the poor yield of valid indents. The residual strength was tested immediately after notching in the same 4pt setup at a fast crosshead speed of 2.5 mm/min to avoid subcritical crack growth effects. The calculation of K_{ISB} was carried out according to Chantikul [28].

Moreover, this dummy indentation method (only one indent leads to fracture) offers the opportunity to calculate the fracture resistance K_{LWN} from the extension of the cracks of the longest surviving cracks. This was carried out by the procedure described by Dransmann [29] assuming a crack geometry factor of $\psi = 0.95$ (This value was chosen after inspecting some fractured bars). Palmqvist cracks are flatter than halfpenny cracks with a geometry factor of $\psi = 1.27$ for which the method was originally designed by Braun and Lawn [30]. The same crack shape correction was also applied to the ISB test.

Finally, the stable indentation crack growth in bending (SIGB) test was carried out with HV10 indents placed at elevated temperature. It is known that the transformability is temperature dependent. Tsai found a complete elimination of transformation in Ce-TZP at 400 °C [11]. The idea was to produce valid indentations with wing cracks exceeding the size of the transformation zone and thereby eliminate crack trapping effects [31]. With respect to the thermal vulnerability of the 1.5Y-TZP material [24] preliminary tests were carried out to identify the correct temperature to reliably induce cracks without damaging the material too much. A heating plate (IKA-Werke, Staufen, Germany) was set to 200 °C and the samples were pre-heated on a zirconia support plate for 15 min. Then the sample was transferred to the indenter device together with the support plate (to prevent too fast cooling) and the four HV10 indents were placed immediately as described above. Temperatures > 200 °C lead to spontaneous transformation. The SIGB test was carried out with an initial bending stress of 400 MPa. Then the stress was increased in 100 MPa increments until sample failure. The crack length was measured after each loading step with the microscope of the hardness machine. The crosshead speed was set to 5 mm/min to avoid subcritical crack growth in the same 4pt test setup.

For evaluation of the SIGB test results, it is assumed that the indenter causes a certain stress intensity which leads to crack opening. After lifting the indenter, a residual (negative!) stress intensity K_{res} is stored in the sample. The indentation cracks are exposed to a total stress intensity K_{tot} which combines K_{res} and the applied stress intensity K_{app} (equation 2).

$$K_{tot} = K_{res} + K_{app} = \chi \cdot P \cdot c^{-1.5} + \psi \cdot \sigma \cdot \sqrt{c} \quad (2)$$

With: P the indentation load, χ the residual stress coefficient, ψ is a geometry factor (e.g. 1.27 for a halfpenny crack), σ the bending stress and c the surface crack length. The onset of crack growth by applied bending stress requires that the applied stress intensity $K_{app} > K_{app,0} = - K_{res}$. With increasing applied stress intensity the crack grows until the sample finally fails. For quantitative evaluation $\psi \cdot \sigma \cdot \sqrt{c}$ is plotted versus $P \cdot c^{-1.5}$. In the resulting plot $\psi \cdot \sigma \cdot \sqrt{c}$ rises at constant crack length until $K_{app} > K_{app,0}$. Then at higher stress intensity the crack starts to grow and the curve rises with a slope χ. In the plot the Y-axis intercept represents the fracture toughness K_{IC} (at infinite crack length) while the kink in the curve represents $K_{app,0}$. $K_{app,0}$ is the R-curve dependent part of the toughness and $K_{I0} = K_{IC} - K_{app,0}$ is the threshold toughness, also called the resistance to subcritical crack growth [29]. With respect to the flat crack profiles a geometry factor of $\psi = 0.95$ was chosen for the evaluation of the plot. Hence, toughness values with crack shape correction are approximately 25 % lower compared to the values assuming semicircular cracks ($\psi = 1.27$).

The SIGB test also allows calculation of R-curves [29]. In case of very steep R-curves the initial region at the onset of crack growth is difficult to investigate by SEVNB tests. For the given material Imariouane determined a plateau toughness after a crack extension of less than 100 µm [23]. The

 doi:10.20944/preprints202407.1207.v1

initial part of the R-curve can be measured according to Anderson [32]. Here bending bars are indented at elevated temperature as before and then annealed at 1150 °C for 5 minutes to revert the phase transformation and eliminate the residual stress caused by the indentations. Such indentation based R-curves typically are measured in two steps: for the initial few microns of crack growth indented and annealed samples are tested (without residual stress $K_{res} = 0$ and $K_{tot} = \psi\sigma\sqrt{c}$), for longer crack lengths $K_{res} \rightarrow 0$; the data from the SIGB tests can be used. Combination of both tests leads to the complete R-curve.

Based on the assumption that the compressive transformation related stress is the main component of the indentation induced residual stress K_{res} in the vicinity of the indent, the notching at elevated temperature will trigger significantly less phase transformation; this should reduce K_{res} and thereby possible crack trapping significantly.

Scanning electron microscopy SEM images of the microstructure were made from polished and thermally etched (1150 °C/5 min, air) surfaces, (FEI Helios nanolab600, Eindhoven, the Netherlands, SE 3kV acceleration voltage). The average grain size was determined by linear intercept method using the correction factor of Mendelson [33].

The tensile sides of the fractured bars were inspected for transformation bands by optical microscopy equipped with differential interference contrast (DIC).

The phase composition was studied by X-Ray diffraction (X'Pert MPD, Panalytical, Eindhoven, the Netherlands, CuKα1, Ge-monochromator, Bragg-Brentano setup, accelerator detector). The samples were studied as-fired after sintering and in polished condition. The fracture surfaces of 4pt bending bars were also inspected. The monoclinic and tetragonal fractions were evaluated by integrating the monoclinic -111 and 111 peaks and the tetragonal 101 peak in the 27–33° 2θ fingerprint range. The volumetric contents were calculated from the peak areas using the calibration curve of Toraya [34]. The transformation zone sizes h were calculated from XRD-Data according to Kosmac [35]. Transformation toughness values were calculated according to McMeeking (equation 1) using a transformation efficiency factor of X = 0.27 [13].

The density of the materials was determined by buoyancy method (Kern&Sohn, Lörrach, Germany).

3. Results

3.1. Mechanical Characterization

Figure 1 shows the Vickers hardness HV10 and the bending strength σ_{4pt}. The hardness stays invariant at 1215 HV10 between 1250–1350 °C sintering temperature and then slightly declines to 1200 HV10 at 1400 °C. The bending strength slightly declines with increasing sintering temperature from 1070 MPa to 1020 MPa. The low scattering of the bending strength at 1250 °C and 1300 °C sintering temperature is noteworthy (only ± 25–40 MPa). The larger scattering at 1350°C is caused by a single sample which exceeded the average strength by more than 200 MPa within a population of samples with ~1000 MPa strength.

Preprints.org (www.preprints.org) | NOT PEER-REVIEWED | Posted: 15 July 2024 doi:10.20944/preprints202407.1207.v1

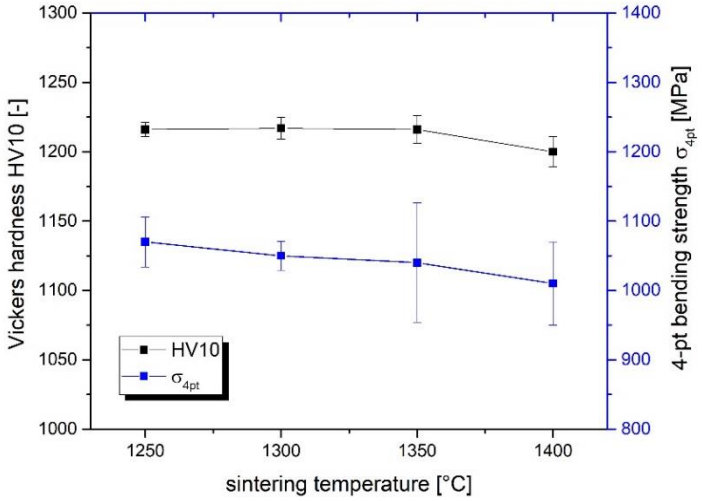

Figure 1. Vickers hardness HV10 and 4-pt bending strength of TZP materials vs. sintering temperature.

Figure 2 shows the stress-deformation curves of the strongest samples of the individual series of 4pt bending tests. Only weak indications of non-linearity were observed in most of the stress-deformation curves. Typically, in the range of 750–850 MPa a slight bending is observed. The slope of the curve does not decline continuously after initiation of transformation as we may expect. The slope remains constant either up to failure, or as in the rare case of a sample sintered at 1350 °C, a second bending event occurs after which the slope continues to decline. The latter effect was, however only observed for a single sample with exceptionally high strength. The majority of samples fails without a second bending event.

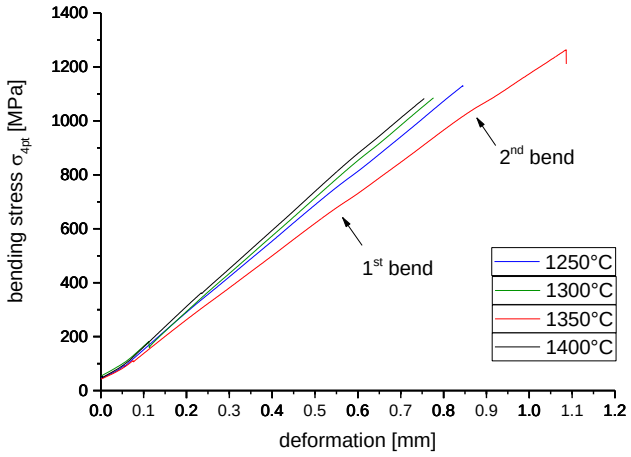

Figure 2. Stress deformation curves of samples with highest strength in 4pt bending tests for each series.

In case of 3pt bending tests (not shown in detail) there is either no observable non-linearity (samples sintered at 1350 °C and 1400 °C) or the non-linearity occurs shortly before failure. Some samples sintered at 1250 °C and 1300 °C show a weak non-linearity at ~ 1000 MPa. The difference between 4pt and 3pt bending tests is probably due to the different volume exposed to constant stress. In case of 4pt bending many transformation bands (see Figure 3) are initiated simultaneously while

 doi:10.20944/preprints202407.1207.v1

in case of 3pt bending initially a single band is produced which leads to a much lower non-linearity which is observable only at high stress.

This assumption is confirmed by the presence of transformation bands on the tensile sides of the bending bars as shown in Figure 3. At low sintering temperatures (1250 °C and 1300 °C) the bands are not very pronounced and rather blurry, at high sintering temperatures (1350 °C and 1400 °C) the bands become more pronounced. The spacing between the bands ranges between 100–400 µm.

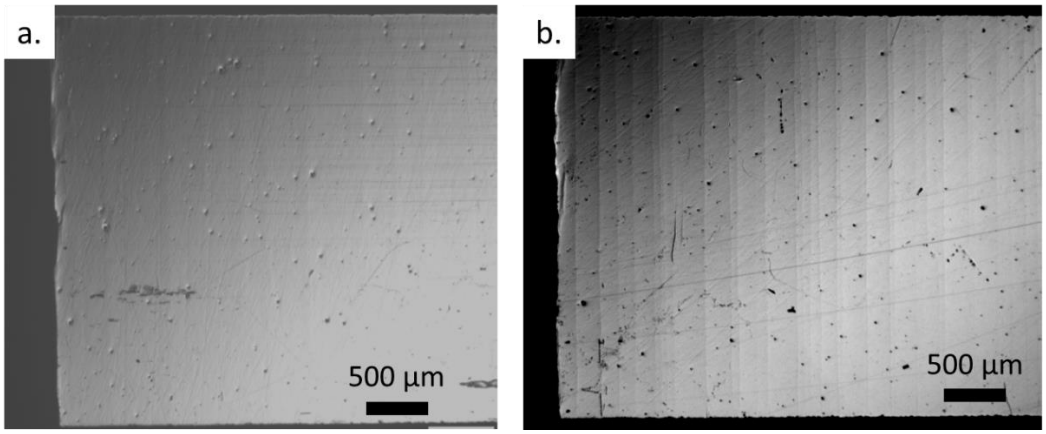

Figure 3. Transformation bands on the tensile side of bars fractured in 4pt bending tests, a. sintered at 1300 °C, b. sintered at 1400 °C, applied bending stress ~1000 MPa.

The transformation stresses measured from the location of bands in samples from 3pt bending tests are shown in Figure 4. The transformation stress decreases with increasing sintering temperature as expected. Note that the transformation stress in 4pt bending is lower.

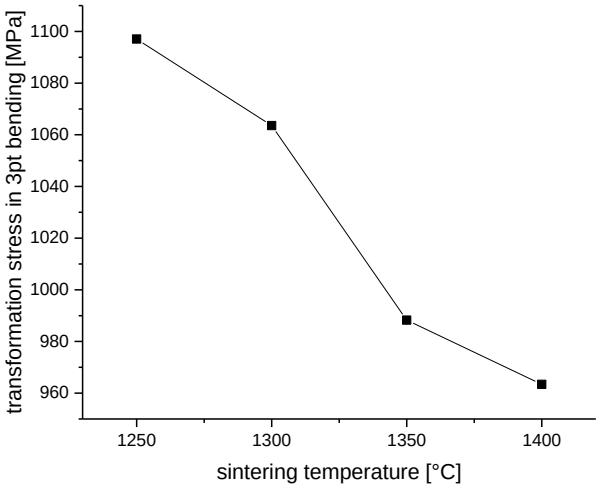

Figure 4. Transformation stress measured from transformation band formation in 3pt bending.

Figure 5 shows the results of the uncorrected DCM and ISB toughness measurements. The K_{DCM} values are extremely high (15–19 MPa√m) and confirm the findings of Matsui [22]. The toughness maximum is found at 1350 °C. With regard to the difficulty to obtain valid indents, it is suspected that trapping of cracks in the transformation zone surrounding the indent is responsible for overestimated toughness values [31]. A priori we should expect an increase in toughness with sintering temperature and grain size. The uncorrected K_{ISB} values (geometry factor ψ = 1.27 for halfpenny crack) are in the range of 14–15 MPa√m and invariant with respect to sintering temperature. Uncorrected K_{LWN} toughness values calculated from the measured stress intensities of

 doi:10.20944/preprints202407.1207.v1

the surviving cracks at dummy indentations are somewhat lower than K_{ISB} values, they also show a toughness maximum at 1350 °C.

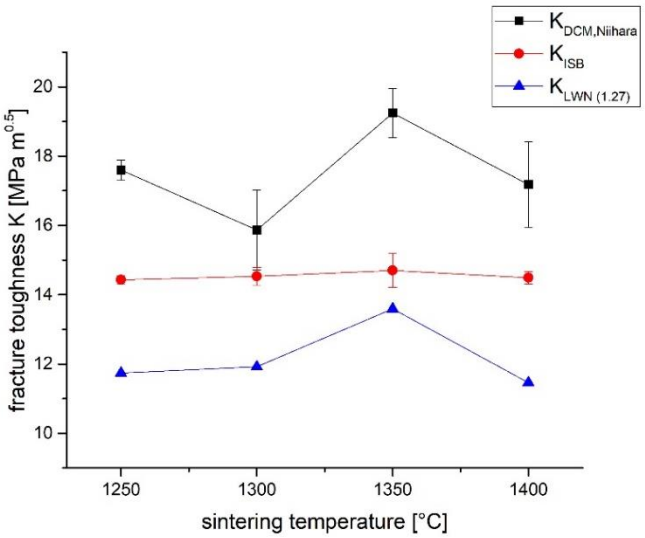

Figure 5. Uncorrected fracture toughness values of TZP materials vs. sintering temperatures temperature determined with different measuring protocols.

An inspection of the fracture surfaces after an ISB test provides evidence that the zone of stable crack extension which has developed from the starter crack introduced by indentation is very flat and not semicircular (Figure 6).

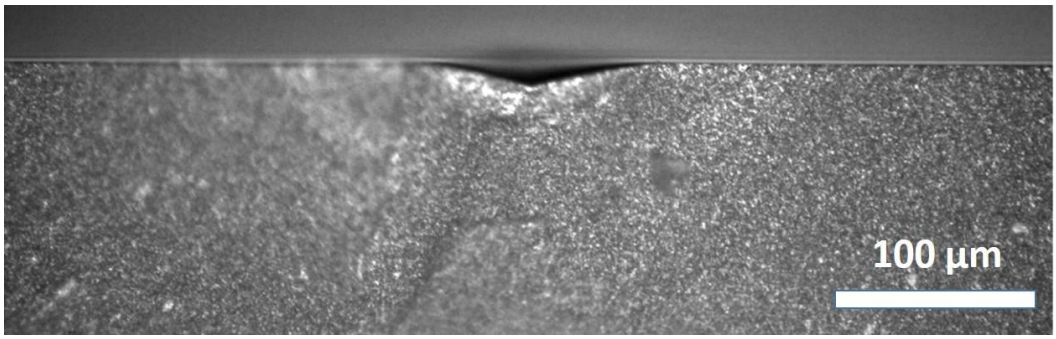

Figure 6. Fracture surface of test bar sintered at 1350 °C, fractured in ISB-test.

The halos of the cracks besides the indents hint at a shallow Palmqvist type crack profile. The lateral extension is larger than the depth. Moreover, the curvature is dented in the region below the indent. A correction of crack geometry factor according to Newman-Raju [36] is required to compensate for the non-semicircular geometry. Dransmann [29] experimentally determined ψ - values of 1.19 and 1.08 for 4Y-TZP and 3Y-TZP by polishing out the indent and studying the crack geometry at different depths during further material removal. This procedure is, however, not applicable in the present case as the cracks are so short that after polishing out the indent virtually nothing will be left. The geometry factor $\psi = 0.95$ was therefore estimated a priori from the crack geometry and contains a certain level of uncertainty.

Figure 7 shows the plots of the SIGB tests carried out with samples indented at 200 °C. Compared to cold indentation the crack length c_0 of the initial crack increases from 135 µm to 155 µm. Evidently the regions beyond $K_{app,0}$ (the linear part of the curve) are well developed. At short crack length a deviation from the ideal behavior is observed, the cracks grow slowly with increasing applied stress intensity. Due to this fading behavior presumably caused by subcritical crack growth, $K_{app,0}$ can therefore not be determined very exactly. In the plots $K_{app,0}$ is in the range between 4–5 MPa$\sqrt{m}$. If an

 doi:10.20944/preprints202407.1207.v1

extrapolation to infinite crack length (which is unrealistic) is avoided, the maximum stress intensity measured for the longest surviving cracks is termed $K_{IC} = K_{LWN}$. Total crack lengths c in most cases do not exceed 0.2 µm, the crack growth $\Delta c = c - c_0$ is in the range of 40–80 µm. With respect to the high crack velocity close to criticality "catching" longer cracks would require significantly larger samples.

The threshold toughness $K_{I0} = K_{LWN} - K_{app,0}$ is therefore in the range between 3.6–5 MPa√m which is quite close or slightly above to the typical value (3–4 MPa√m) for Y-TZP materials [37]. This result is in accord with Imariouane's double torsion results [23].

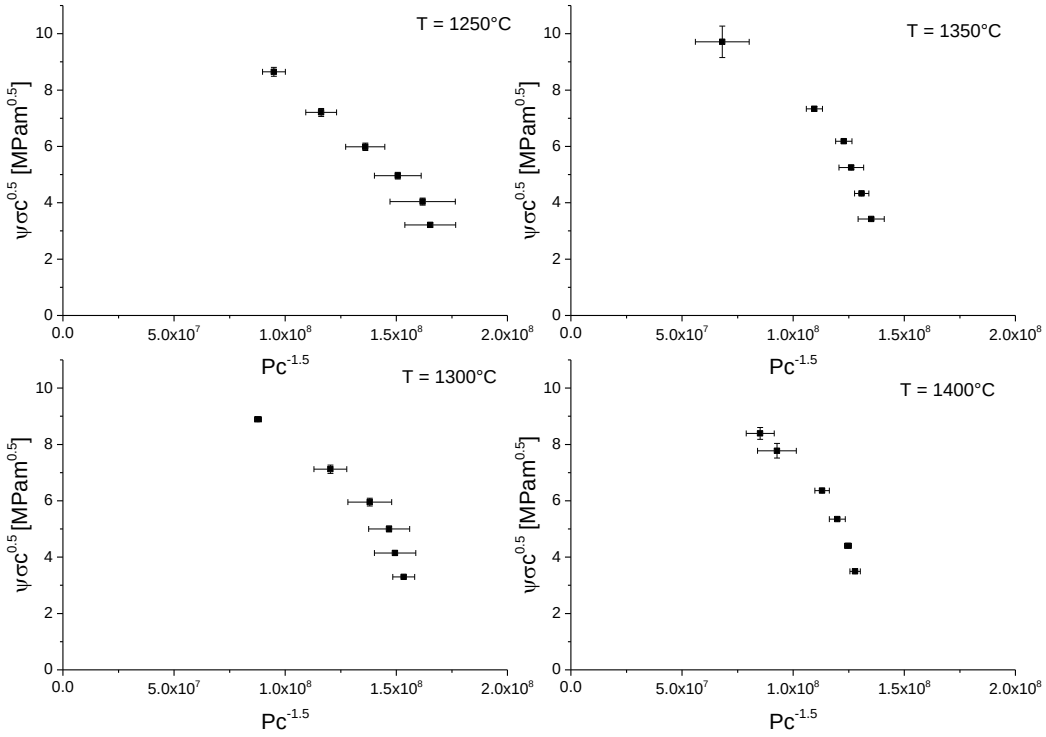

Figure 7. Plots of SIGB tests (average values from 4 series of indents).

The K_{LWN}, $K_{app,0}$ and K_{I0} values corrected for flatter crack geometry (geometry factor $\psi = 0.95$) are shown in Figure 8. The corrected K_{ISB} and K_{LWN} values are considerably lower (~9–10 MPa√m) and in the range of the SEVNB and double torsion test toughness values. Assuming $K_{IC} = K_{LWN}$ the measured values for the resistance to subcritical crack growth K_{I0} and fracture toughness K_{LWN} imply that the fatigue strength values $\sigma_{FS} = \sigma_{4pt} \cdot K_{I0}/K_{IC}$ are in the range of 450–500 MPa for all sintering temperatures.

Preprints.org (www.preprints.org) | NOT PEER-REVIEWED | Posted: 15 July 2024 doi:10.20944/preprints202407.1207.v1

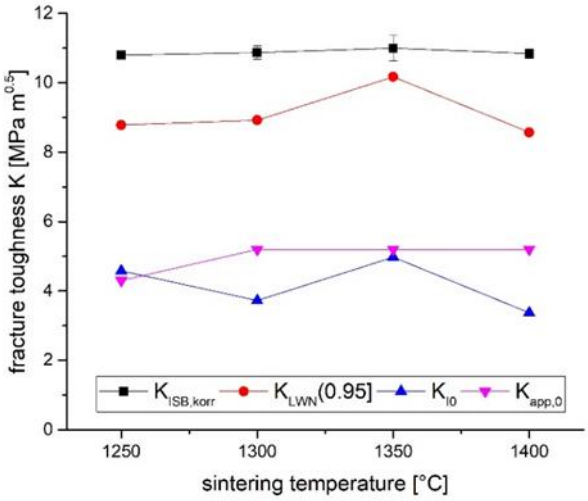

Figure 8. Corrected toughness values K_{ISB}, K_{LWN}, $K_{app,0}$ and K_{I0} assuming a crack geometry factor of 0.95.

According to literature SEVNB tests show a steep increase of toughness to a plateau value of ~8.5 MPa√m within the first 100 µm of crack extension, double torsion tests show toughness values of up to 9.5–10 MPa√m under fast fracture conditions [23]. A more detailed statement concerning shorter cracks is not possible with SEVNB method. SIGB tests with annealed and non-annealed samples were combined to construct the R-curves [29,32] in the crack length range between 0-50 µm (Figure 9). The results show that the toughness K_0 at zero crack extension is 3–3.2 MPa√m, the R-curve dependent part of toughness is in the range of 5.5–6 MPa√m which is in good accord with the SIGB results. The R-curves become steeper with increasing sintering temperature. It seems, however, that the curves did not reach the saturation level yet.

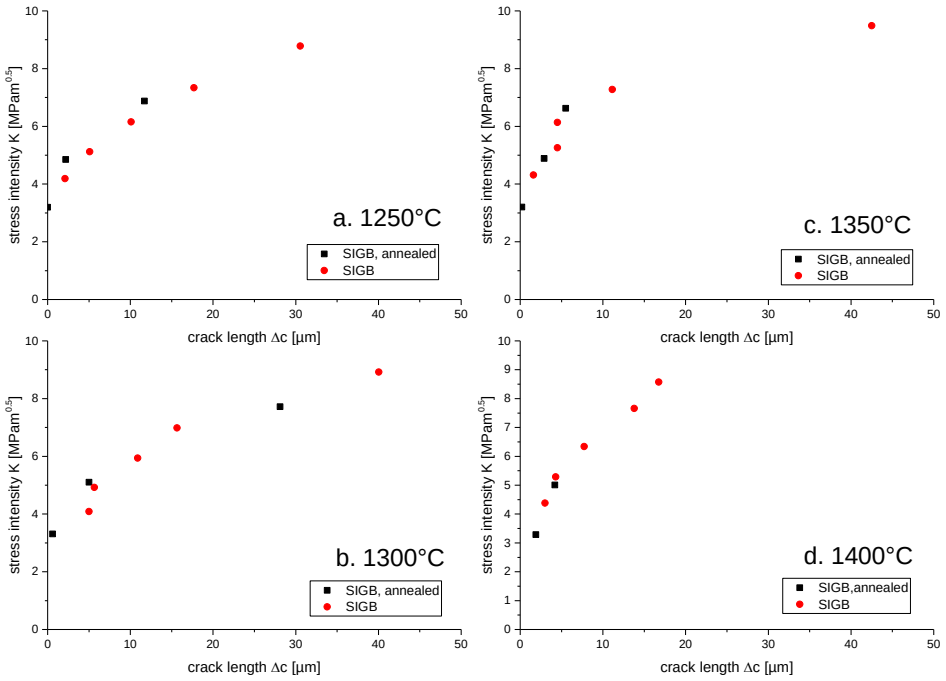

Figure 9. Plots of SIGB tests (average values from 4 series of indents).

 doi:10.20944/preprints202407.1207.v1

3.2. Phase Composition

The materials were entirely tetragonal after sintering. Neither monoclinic peaks nor cubic peaks were detected. The phase composition of the fracture surfaces showed very uniform values of 80–81 vol% monoclinic, this is very close to the theoretical maximum transformable content of 85–90 vol% [38]. Consequently, the transformation zone sizes h calculated according to Kosmac [35] were also extremely uniform with values of h = 3.3–3.4 µm. The calculated transformation toughness values ΔK_{IC}^{T} according to McMeeking [13] (with X = 0.27) were between 4.76–4.96 MPa√m. The maximum values for h and ΔK_{IC}^{T} were obtained for the sample sintered at 1350 °C. The transformation toughness values fit very well with the data from the SIGB test assuming that $K_{app,0}$ corresponds to the toughness increments contributed by reinforcement mechanisms (in this case only transformation toughening).

3.3. Microstructure

Figure 10 shows SEM images of the polished and thermally etched surfaces of 1.5Y-TZP samples sintered at the four different temperatures. The microstructure is dense and homogeneous. Grain growth with increasing sintering temperature seems very moderate.

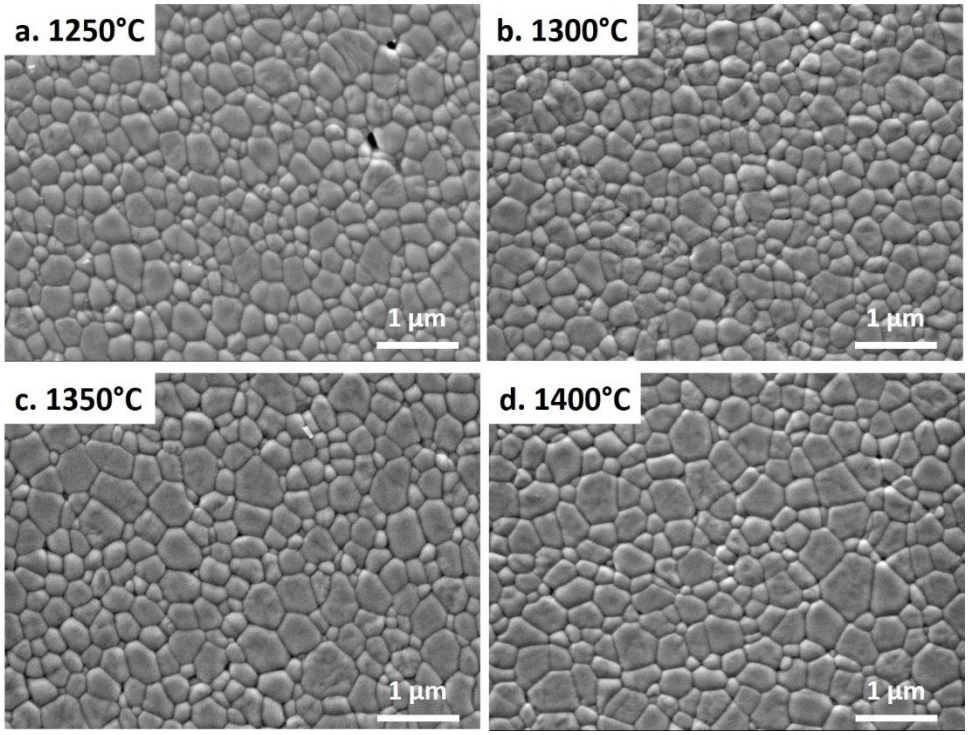

Figure 10. Microstructure of 1.5Y-TZP sintered at different temperatures. SEM images of polished thermally etched surfaces.

Figure 11 shows the grain sizes determined by linear intercept method including a geometry correction factor of 1.56 [33]. Grain growth with increasing sintering temperature is clearly visible. Samples sintered at 1250 °C have an average grain size of 320 nm, the grain size increases to 450 nm at a sintering temperature of 1450 °C. Note that the given standard deviation is not the deviation in grain size (which systematically cannot be determined by linear intercept method as grains are sectioned at different levels) but the deviation within five measurements.

 doi:10.20944/preprints202407.1207.v1

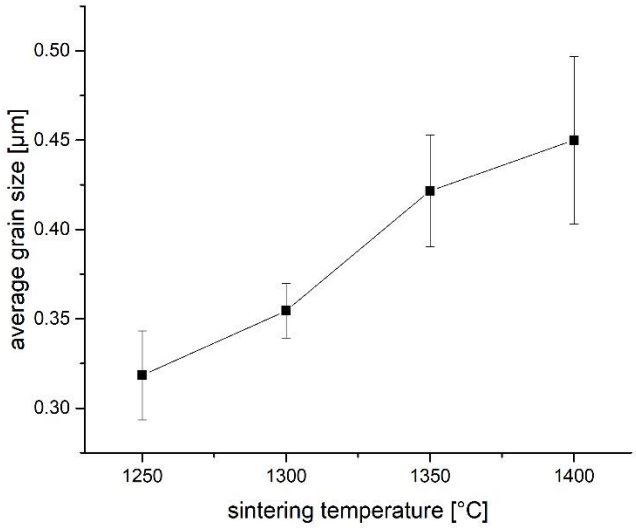

Figure 11. Average corrected grain size of 1.5Y-TZP vs. sintering temperature.

4. Discussion

1.5Y-TZP materials were manufactured by axial pressing of commercially available RTP powders. Materials were characterized with respect to microstructure, transformation characteristics and mechanical properties. The materials show a combination of high strength and toughness within a relatively broad processing temperature field of 1250–1400 °C. The study allowed to re-evaluate the previous publications by Matsui and Imariouane [22,23] using the same starting powder but slightly different processing conditions.

The extremely high stress induced transformability of the materials (> 80 % phase transformation in fracture surfaces) guarantees a high damage tolerance. Samples sintered at 1250–1300 °C showed almost no scattering in their strength data. Simultaneously the high transformability seems to be the reason for over-estimation of fracture toughness by direct crack length measurement. Quinn and Bradt [39] have banned direct crack length measurements in general due to unclear criteria for crack arrest. This popular technique is however very fast and easy to apply. In fact, for small samples there are not many alternatives. In the present case using DCM definitely cannot be recommended.

The reason for the over-estimated DCM toughness values for 1.5Y-TZP [20–22] seems to be material specific. Indentation causes phase transformation around the indent which, due to volume expansion of the material, prevents crack growth extremely efficiently. Hence, cracks are trapped and regular crack patterns are seldom obtained. This phenomenon was described by Cook for 3Y-TZP materials [31]. Our experience is however that in case of the less transformable 3Y-TZP the trapping problem can be avoided if sample preparation is gentle and automated in order to avoid residual stress introduced by the final machining process.

This intense transformation behavior also affects toughness measurements from residual strength measurements if samples are notched with Vickers indents at ambient temperature. Residual strength levels in such ISB-tests may reach almost 1000 MPa and are therefore only marginally lower than the strength of the pristine samples. Surviving cracks of multiple indentations either grow and the sample fails at this indent or they are trapped and only little crack growth is observed. In its extreme case the crack requires such a high stress intensity to exit the trapping zone that, once the region outside the zone is reached, immediate failure occurs. An indentation crack trapped by compressive stress in the transformation zone cannot be compared to a natural flaw where the transformation zone is built up during crack growth and where much more pronounced crack growth can be expected.

 doi:10.20944/preprints202407.1207.v1

Indentation at elevated temperature can help to produce more regular crack patterns. Cracks introduced by HV10 indentations at 200 °C extend 20 μm further than cracks induced at room temperature. The required applied stress to let them grow is reduced; simultaneously the transformation around the indent is suppressed. In combination this means a reduction of K_{res} which results in regular crack patterns with four well developed wing cracks of equal length. This facilitates SIGB tests and introduces more statistical quality, typically all perpendicular crack pairs grow with increasing applied stress and can be measured. In cold indented materials it happens frequently that only one crack is "running" while the others remain trapped.

However, the temperature for hot indentation has to be chosen with care. In case of the 1.5Y-TZP material tested in this study (which was known to be thermally vulnerable [24]) notching at 250 °C leads to spontaneous uncontrolled transformation of the material surrounding the indent, so that not only wing cracks but also cracks from the sides of the indents are produced. Transferring the method to other materials with high transformability therefore should be done with care and the appropriate temperatures should be checked by preliminary experiments. The comparison with the results of Imariouane [23] shows that the modified indentation methodology seems valid to determine the toughness of this highly transformable material reliably. The slight reduction of toughness and strength in the TZP sintered at 1400 °C/2 h compared to TZPs sintered at lower temperature indicates that this material is very close to the critical grain size.

The relatively weak non-linearity of stress-deformation curves of 4pt bending tests is evident. We can, however, only speculate why the slope of the stress-deformation curves does not decline continuously after triggering the phase transformation. Transformation is initiated when a certain population of large grains reaches its critical transformation stress. The transformation bands are known to exert a certain stress shielding effect in their vicinity which prevents formation of new bands close to the initial ones [25]. This may restore the rigidity of the material until the stress is high enough to either lead to failure (the common case) or to formation of new bands while the sample survives up to a somewhat higher stress (only observed in a single case). In case of 3pt bending with a localized high stress, only single bending events occur close to the failure stress.

The calculated transformation toughness values (approximately 5 MPa√m), the $K_{app,0}$ values of SIGB tests which represent the R-curve dependent part of toughness (5 MPa√m) and the R-curve related part of toughness obtained directly from R-curves (5.5–6 MPa√m) agree very well. It is assumed that transformation toughening is the only relevant toughening mechanism. According to Swain the maximum toughness allowed for flaw size related failure in Y-TZP is ~7.5 MPa√m [12]. Consequently, depending on the K_0 value (4 MPa√m acc. to Swain, 3 MPa√m measured in this study) the R-curve related toughness should not be higher than 3.5–4.5 MPa√m. The R-curve related toughness measured in this study (5-6 MPa√m depending on the method used) is well above this level. Transformation related failure is confirmed by formation of transformation bands prior to failure. Transformation bands are however very narrow and start to occur at a stress slightly below the failure stress. This explains why a high strength level can be maintained. Macroscopic non-linearity of stress-strain curves was only observed in a few samples with relatively high strength. Typically, samples fail upon reaching the critical transformation stress.

These tough 1.5Y-TZP materials offer a very narrow and reliable strength distribution and high safety in case of catastrophic events. Under fatigue load conditions their relatively unfavorable K_{I0}/K_{IC} ratio allows constant stress levels not higher than 450–500 MPa to prevent fatigue failure. With respect to sintering temperature and LTD resistance reported in literature [24] it is probably advisable not to fully exploit the potential toughness and to choose a sintering temperatures not higher than 1300 °C at 2 h dwell. Moreover, it has to be stated that this 1.5Y-TZP is a material to be applied at ambient temperature, exposition to elevated temperatures for a prolonged time should be avoided.

5. Conclusions

The present study shows that 1.5Y-TZP materials offer a favorable combination of high strength of 1000 MPa and a fracture toughness of 8–10 MPa√m. The materials are therefore attractive in applications which require high damage tolerance in catastrophic events rather than high fatigue

strength. Users aiming to apply these understabilized TZPs should be aware of the specific advantages and drawbacks of these materials, even more so as direct crack length measurements lead to an extreme overestimation of toughness. This may lead to fatal errors in design of components. An alternative indentation based method, SIGB, using indents placed at elevated temperature, is able to reliably reproduce the toughness values measured by conservative methods. Transformation toughness seems to be the only toughening mechanism active in these materials. R-curve related toughness increments determined by different measuring protocols are in excellent agreement with calculated transformation toughness values from XRD measurements.

Author Contributions: Conceptualization, F.K.; investigation F.K. and B.O.; writing—original draft preparation, F.K.; writing—review and editing, F.K. and B.O.; visualization, B.O. All authors have read and agreed to the published version of the manuscript.

Funding: This research received no external funding.

Data Availability Statement: The raw data supporting the conclusions of this article will be made available by the authors on request.

Conflicts of Interest: The authors declare no conflicts of interest.

References

1. Evans, A.G. Perspective on the Development of High-Toughness Ceramics. *Journal of the American Ceramic Society* **1990**, *73*, 187–206.
2. Rose, L.R.F. The mechanics of transformation toughening. *Proc. R. Soc. Lond. A* **1987**, *412*, 169–197, doi:10.1098/rspa.1987.0084.
3. Hannink, R.H.J.; Kelly, P.M.; Muddle, B.C. Transformation Toughening in Zirconia-Containing Ceramics. *Journal of the American Ceramic Society* **2000**, *83*, 461–487, doi:10.1111/j.1151-2916.2000.tb01221.x.
4. Li, P.; Chen, I.-W.; Penner-Hahn, J.E. Effect of Dopants on Zirconia Stabilization - An X-ray Absorption Study: II, Tetravalent Dopants. *Journal of the American Ceramic Society* **1994**, *77*, 1281–1288.
5. Li, P.; Chen, I.-W.; Penner-Hahn, J.E. Effect of Dopants on Zirconia Stabilization - An X-ray Absorption Study: I, Trivalent Dopants. *Journal of the American Ceramic Society* **1994**, *77*, 118–128.
6. Kelly, J.R.; Denry, I. Stabilized zirconia as a structural ceramic: An overview. *Dent. Mater.* **2008**, *24*, 289–298, doi:10.1016/j.dental.2007.05.005.
7. Tsukuma, K.; Shimada, M. Strength, fracture toughness and Vickers hardness of CeO_2-stabilized tetragonal ZrO_2 polycrystals (Ce-TZP). *Journal of Materials Science* **1985**, *20*, 1178–1184, doi:10.1007/BF01026311.
8. Kelly, P.M.; Rose, L.R.F. The martensitic transformation in ceramics — its role in transformation toughening. *Progress in Materials Science* **2002**, *47*, 463–557, doi:10.1016/S0079-6425(00)00005-0.
9. REYES-MOREL, P.E.; Chen, I.-W. Transformation Plasticity of CeO 2 -Stabilized Tetragonal Zirconia Polycrystals: I, Stress Assistance and Autocatalysis. *J Am Ceram Soc* **1988**, *71*, 343–353, doi:10.1111/j.1151-2916.1988.tb05052.x.
10. Yu, C.-S.; Shetty, D.K. Transformation yielding, plasticity and crack-growth-resistance (R-curve) behaviour of CeO2-TZP. *J Mater Sci* **1990**, *25*, 2025–2035, doi:10.1007/BF01045759.
11. Tsai, J.-F.; Shetty, D.K. Cyclic Fatigue of Ce-TZP/AI 2 O 3 Composites: Role of the Degradation of Transformation Zone Shielding. *J Am Ceram Soc* **1995**, *78*, 599–608, doi:10.1111/j.1151-2916.1995.tb08221.x.
12. Swain, M.V.; Rose, L.R.F. Strength Limitations of Transformation-Toughened Zirconia Alloys. *Journal of the American Ceramic Society* **1986**, *69*, 511–518.
13. McMeeking, R.M.; Evans, A.G. Mechanics of Transformation-Toughening in Brittle Materials. *Journal of the American Ceramic Society* **1982**, *65*, 242-246.
14. Lange, F.F. Transformation toughening: Part 1 Size effects associated with the thermodynamics of constrained transformations. *Journal of Materials Science* **1982**, *17*, 225–234, doi:10.1007/BF00809057.
15. Swain, M.V. Grain-size dependence of toughness and transformability of 2mol% Y-TZP ceramics. *Journal of Materials Science Letters* **1986**, *5*, 1159–1162, doi:10.1007/BF01742233.
16. Ruiz, L.; Readey, M.J. Effect of Heat Treatment on Grain Size, Phase Assemblage, and Mechanical Properties of 3 mol% Y-TZP. *J Am Ceram Soc* **1996**, *79*, 2331–2340, doi:10.1111/j.1151-2916.1996.tb08980.x.
17. Lange, F.F. Transformation toughening: Part 3 Experimental observations in the ZrO_2- Y_2O_3 system. *Journal of Materials Science* **1982**, *17*, 240–246.
18. Chen, M.; Hallstedt, B.; Gauckler, L.J. Thermodynamic modeling of the ZrO_2–$YO_{1.5}$ system. *Solid State Ionics* **2004**, *170*, 255–274, doi:10.1016/j.ssi.2004.02.017.
19. Matsui, K.; Yoshida, H.; Ikuhara, Y. Phase-transformation and grain-growth kinetics in yttria-stabilized tetragonal zirconia polycrystal doped with a small amount of alumina. *Journal of the European Ceramic Society* **2010**, *30*, 1679–1690, doi:10.1016/j.jeurceramsoc.2010.01.007.

 doi:10.20944/preprints202407.1207.v1

20. Bravo-Leon, A.; Morikawa, Y.; Kawahara, M.; Mayo, M.J. Fracture toughness of nanocrystalline tetragonal zirconia with low yttria content. *Acta Materialia* **2002**, *50*, 4555–4562, doi:10.1016/S1359-6454(02)00283-5.
21. Binner, J.; Vaidhyanathan, B.; Paul, A.; Annaporani, K.; Raghupathy, B. Compositional Effects in Nanostructured Yttria Partially Stabilized Zirconia. *International Journal of Applied Ceramic Technology* **2011**, *8*, 766–782, doi:10.1111/j.1744-7402.2010.02503.x.
22. Matsui, K.; Hosoi, K.; Feng, B.; Yoshida, H.; Ikuhara, Y. Ultrahigh toughness zirconia ceramics. *Proc. Natl. Acad. Sci. U. S. A.* **2023**, *120*, e2304498120, doi:10.1073/pnas.2304498120.
23. Imariouane, M.; Saâdaoui, M.; Denis, G.; Reveron, H.; Chevalier, J. Low-yttria doped zirconia: Bridging the gap between strong and tough ceramics. *Journal of the European Ceramic Society* **2023**, *43*, 4906–4915, doi:10.1016/j.jeurceramsoc.2023.04.021.
24. Imariouane, M.; Saâdaoui, M.; Cardinal, S.; Reveron, H.; Chevalier, J. Aging behavior of a 1.5 mol% yttria doped zirconia exhibiting optimized toughness and strength. *Journal of the European Ceramic Society* **2024**, *44*, 1053–1060, doi:10.1016/j.jeurceramsoc.2023.09.041.
25. Kern, F.; Osswald, B. Properties of a Pressureless Sintered 2Y-TZP Material Combining High Strength and Toughness. *Ceramics* **2024**, *7*, 893–905, doi:10.3390/ceramics7030058.
26. Liens, A.; Swain, M.; Reveron, H.; Cavoret, J.; Sainsot, P.; Courtois, N.; Fabrègue, D.; Chevalier, J. Development of transformation bands in ceria-stabilized-zirconia based composites during bending at room temperature. *Journal of the European Ceramic Society* **2021**, *41*, 691–705, doi:10.1016/j.jeurceramsoc.2020.08.062.
27. Niihara, K.; Morena, R.; Hasselman, D.P.H. Evaluation of K_{Ic} of brittle solids by the indentation method with low crack-to-indent ratios. *Journal of Materials Science Letters* **1982**, *1*, 13–16, doi:10.1007/BF00724706.
28. Chantikul, P.; Anstis, G.R.; Lawn, B.R.; Marshall, D.B. A Critical Evaluation of Indentation Techniques for Measuring Fracture Toughness: II, Strength Method. *Journal of the American Ceramic Society* **1981**, *64*, 539–543, doi:10.1111/j.1151-2916.1981.tb10321.x.
29. Dransmann, G.W.; Steinbrech, R.W.; Pajares, A.; Guiberteau, F.; Dominguez-Rodriguez, A.; Heuer, A.H. Indentation Studies on Y2O3-Stabilized ZrO2: II, Toughness Determination from Stable Growth of Indentation-Induced Cracks. *J American Ceramic Society* **1994**, *77*, 1194–1201, doi:10.1111/j.1151-2916.1994.tb05392.x.
30. Braun, L.M.; Bennison, S.J.; Lawn, B.R. Objective Evaluation of Short-Crack Toughness Curves Using Indentation Flaws: Case Study on Alumina-Based Ceramics. *Journal of the American Ceramic Society* **1992**, *75*, 3049–3057, doi:10.1111/j.1151-2916.1992.tb04385.x.
31. Cook, R.F.; Braun, L.M.; Cannon, W.R. Trapped cracks at indentations: Part I: Experiments on yttria-tetragonal zirconia polycrystals. *Journal of Materials Science* **1994**, *29*, 2133–2142, doi:10.1007/BF01154700.
32. Anderson, R.M.; Braun, L.M. Technique for the R-Curve Determination of Y-TZP Using Indentation-Produced Flaws. *J Am Ceram Soc* **1990**, *73*, 3059–3062, doi:10.1111/j.1151-2916.1990.tb06716.x.
33. Mendelson, M.I. Average Grain Size in Polycrystalline Ceramics. *Journal of the American Ceramic Society* **1969**, *52*, 443–446, doi:10.1111/j.1151-2916.1969.tb11975.x.
34. Toraya, H.; Yoshimura, M.; Somiya, S. Calibration Curve for Quantitative Analysis of the Monoclinic-Tetragonal ZrO_2 System by X-Ray Diffraction. *Journal of the American Ceramic Society* **1984**, *67*, C119-C121, doi:10.1111/j.1151-2916.1984.tb19715.x.
35. Kosmać, T.; Wagner, R.; Claussen, N. X-Ray Determination of Transformation Depths in Ceramics Containing Tetragonal ZrO_2. *Journal of the American Ceramic Society* **1981**, *64*, C-72-C-73, doi:10.1111/j.1151-2916.1981.tb10285.x.
36. Newman, J.C.; Raju, I.S. Analyses of Surface Cracks in Finite Plates Unter Tension or Bending Loads. *Nasa Technical Paper* **1979**, *1578*.
37. Chevalier, J.; Saadaoui, M.; Olagnon, C.; Fantozzi, G. Double-torsion testing a 3Y-TZP ceramic. *Ceramics International* **1996**, *22*, 171–177, doi:10.1016/0272-8842(95)00076-3.
38. Mamivand, M.; Asle Zaeem, M.; El Kadiri, H. Phase field modeling of stress-induced tetragonal-to-monoclinic transformation in zirconia and its effect on transformation toughening. *Acta Materialia* **2014**, *64*, 208–219, doi:10.1016/j.actamat.2013.10.031.
39. Quinn, G.D.; Bradt, R.C. On the Vickers Indentation Fracture Toughness Test. *Journal of the American Ceramic Society* **2007**, *90*, 673–680, doi:10.1111/j.1551-2916.2006.01482.x.